OXFORD

Human Molecular Genetics, 2022, Vol. 31, 24, 4241–4254

https://doi.org/10.1093/hmg/ddac177
Advance access publication date 29 July 2022
Original Article

Identification of new RAD51D-regulating microRNAs that also emerge as potent inhibitors of the Fanconi anemia/homologous recombination pathways

Nina Hater[1], Katharina M. Iwaniuk[1], Carina Leifeld[1], Pia Grüten[1], Constanze Wiek[2], Katharina Raba[1], Fan Zhang[3], Johannes C. Fischer[1], Paul R. Andreassen[3,4], Helmut Hanenberg[2,5,†] and Hans-Ingo Trompeter[1,†,*]

[1]Institute for Transplantation Diagnostics and Cell Therapeutics, University Hospital Düsseldorf, Heinrich Heine University, D-40225 Düsseldorf, Germany
[2]Department of Otorhinolaryngology & Head/Neck Surgery, University Hospital Düsseldorf, Heinrich Heine University, D-40225 Düsseldorf, Germany
[3]Division of Experimental Hematology and Cancer Biology, Cincinnati Children's Hospital Medical Center, Cincinnati, OH 45229, USA
[4]Department of Pediatrics, University of Cincinnati College of Medicine, Cincinnati, OH 45229, USA
[5]Department of Pediatrics III, University Children's Hospital Essen, University Duisburg-Essen, D-45147 Essen, Germany

*To whom correspondence should be addressed. Tel: +49 211 8118751; Fax: +49 211 8119109; Email: hans-ingo.trompeter@med.uni-duesseldorf.de

†Both authors contributed equally to this work.

Abstract

The Fanconi anemia (FA) and homologous recombination (HR) pathways, which partially overlap and include RAD51 and its paralogs, are key for the repair of different types of DNA damage, such as DNA interstrand crosslinks. First, to broadly assess the impact of microRNA-mediated regulation, we examined microRNA expression profiles in five isogenic fibroblast cell pairs, either deficient in DNA repair due to germline mutations in *FANCA*, *FANCB*, *FANCC*, *FANCI* or *BRIP1/FANCJ* or proficient due to correction with retroviral vectors. In each pair, we observed lower abundance of specific microRNAs in the FA-deficient cells. From the list of microRNAs, we experimentally confirmed the effects of miR-141-3p and miR-369-3p targeting *RAD51B* and miR-15a-5p, miR-494-3p as well as miR-544a targeting *RAD51D*. However, by western blotting, only RAD51D protein was reduced by a mixture of its regulating microRNAs. Gene ontology analyses and identification of additional FA/HR factors as targets of miR-15a-5p, miR-494-3p and miR-544a strongly suggested the widespread influence of these microRNAs on HR. Interestingly, only miR-494-3p directly reduced RAD51 foci formation, while a mixture of miR-15a-5p, miR-494-3p and miR-544a strongly reduced HR activity in green fluorescent protein (GFP) repair assays. In summary, by successfully employing this novel loss- and gain-of-function strategy, we have identified new microRNAs strongly inhibiting HR in mammalian cells. Understanding and modulating such miRNA regulation of DNA repair genes/pathways might help to overcome the reduced repair capacity of FA patients with biallelic hypomorphic mutations or help to engineer synthetic lethality strategies for patients with mutations in cancer-associated FA/HR genes.

Introduction

MicroRNAs (miRNAs) play a vital role in posttranscriptional gene regulation in eukaryotic cells and are expressed as single-stranded (ss) RNA molecules with an average length of 22 nucleotides (nt) (1). They primarily function by sequence-specific binding to 3'-UTRs of mRNAs resulting in translational inhibition of these targeted transcripts (1). One miRNA can regulate multiple target mRNAs and vice versa; thus, their function should be viewed in a network-regulating manner (2,3). As miRNAs are often expressed in stage- and tissue-specific patterns during development and also during normal cellular function, they can influence a great variety of biological processes including apoptosis, cancer, proliferation, development and differentiation (4–7). Mechanistically, miRNAs are transcribed as primary miRNAs, which are sequentially processed by the RNAses Drosha and Dicer to eventually produce short double-stranded RNA molecules (8,9). One or both of these strands are then incorporated into RNA-induced silencing complexes (RISCs), where binding to the 3'-UTR of the target gene(s) and thereby translational inhibition occurs (1).

The Fanconi Anemia (FA) pathway and the partially overlapping homologous recombination (HR) pathway are key components for the error-free repair of DNA double-strand breaks (DSB) and/or stalled replications forks at DNA interstrand cross-links (ICLs) (10). FA is an autosomal or X-linked-inherited bone marrow failure syndrome caused by germ-line mutations in at least 22 known FA genes linked to DNA ICL repair (10). FA is clinically characterized by congenital abnormalities, progressive bone marrow failure and a high propensity for developing malignancies, predominantly myelodysplastic syndrome / acute myeloid leukemia (MDS/AML) and solid tumors, especially squamous cell carcinomas of the head and neck as well as the anogenital region (11). Cells from FA patients are characteristically hypersensitive to DNA-crosslinking agents, such as busulphan, mitomycin C and cisplatin (12).

The primary function of the FA/HR biochemical network is the removal of DNA ICLs, which are a major obstacle in replication and transcription (13). Mechanistically, ICLs are detected by the FANCM/MHF1/MHF2 complex together with UHRF1 (10,13). Subsequently, the FA core complex, consisting of at least of 10 FA-associated proteins (FANCA, FANCB, FANCC,

Received: March 28, 2022. **Revised:** June 28, 2022. **Accepted:** July 27, 2022

FANCE, FANCF, FANCG, FANCL, FAAP100, FAAP20 and FAAP24), is recruited to repair foci at cross-links and facilitates the monoubiquitination of the FANCD2 and FANCI proteins in interaction with FANCT (UBE2T) (10,13,14). Monoubiquitinated and phosphorylated FANCD2 and FANCI are then recruited as dimers to DNA cross-link sites, leading to the stabilization of stalled replication forks and guiding downstream error-free ICL repair mediated by XPF/ERCC1, MUS81/EME1, FAN1, SLX1 and SLX4 (FANCP). Upon translesion synthesis by POLζ/REV1, DSB repair by HR involves end resection at DSBs, which is initiated by the MRE11/RAD50/NBS1 (MRN) complex and then extended by EXO1/BLM/DNA2 (10,13,15). This processing of the DNA leads to ssDNA overhangs which are protected from degradation by binding to replication protein A (RPA) and which are subsequently loaded with RAD51 monomers that displace RPA to form a nucleoprotein filament structure (a process that leads to RAD51/FANCR foci formation). This step is largely dependent on the FA proteins BRCA2/FANCD1, BRCA1/FANCS and PALB2/FANCN (16,17), which act downstream of monoubiquitinated FANCD2. Formation of these RAD51 filament structures is also supported by complexes of the RAD51 paralogs RAD51B, RAD51C/FANCO, RAD51D, XRCC2/FANCU and XRCC3 (18). The nucleoprotein filament then invades a homologous double-stranded template DNA, thereby establishing a double Holliday structure (16,17). Branch migration is promoted by RAD54, and the subsequent resolution of the Holliday structure is facilitated by GEN1 or the SLX1/4 complex. The CX3-complex formed by two RAD51 paralogs, RAD51C and XRCC3, supports the resolution of Holliday junctions during the final stage of HR (16,17). In line with their pivotal roles in HR, RAD51 and its paralogs are involved in ovarian and breast cancer predisposition (19). A contribution to ovarian cancer development is described for RAD51B (20), RAD51C (21) and RAD51D (22), and breast cancer predisposition is known for RAD51B (20) as well as for XRCC2 (23).

Compared to other biological processes, surprisingly sparse information is available on the regulatory influence of miRNAs on members of the FA/HR pathways. In general, Dicer is required for maintaining genomic stability (24) and the miRNAs from the embryonic stem cell-enriched miR-302 cluster can affect a central step in FA/HR repair, the monoubiquitination of FANCD2 (25). Other miRNAs like miR-23a, miR-146a/b, miR-96, miR-155 or miR-34a can also affect HR by inhibiting target genes such as *BRCA1*, *RAD51* and *FANCG* (26–30). Additionally, miR-103 and miR-107 were shown to directly regulate RAD51 as well as RAD51D and thereby affect HR (31). More recently, miR-200c, an otherwise important regulator of epithelial-mesenchymal transition due to targeting the transcription factors ZEB1 and ZEB2, was suggested to influence the FA/HR pathways downstream of FANCD2 (32).

In this study, we combined bioinformatic analyses with a novel comparative gain-and-loss-of-function approach to identify differential miRNA expression in isogenic cell pairs, each deficient and proficient for a specific FA gene, leading to the identification of new RAD51B and RAD51D regulating miRNAs. From gene ontology (GO) evaluation, foci formation analyses, as well as *bona fide* standard DNA repair assays, the RAD51D regulating miRNAs miR-15a-5p, miR-494-3p and miR-544a emerged as potent inhibitors of the function of the entire FA/HR pathway.

Results

Identification of putative FA-regulating miRNAs

To estimate the potential impact of various miRNAs on members of the FA/HR pathway, we initially performed a bioinformatic prediction survey for the first 20 of the 22 known FA genes (all except *REV7/FANCV* and *RFWD3/FANCW*, and for all 5 somatic RAD51 paralog genes; predictions were made for 23 genes in total). Using the webtool miRWalk 2.0 (33), we integrated results from 6 of the 12 embedded algorithms, namely miRanda (34), PicTar-2 (35), TargetScan (36), miRDB (37), RNA22 (38) and miRWalk (33). As summarized in Figure 1, the predicted miRNA interactions affect all members of the FA/HR pathway analyzed and varied from 107 miRNAs as putative regulators of *FANCB* (bearing a short 160 nt 3'-UTR) to 1696 miRNAs that potentially regulate ERCC4 (4005 nt 3'-UTR). In addition, as detailed in Supplementary Material, Table S1, many miRNAs were predicted to target a high number of FA genes in parallel (637 miRNAs were predicted to target > 10 FA genes). Based on our own experience that approximately 20–30% of predicted miRNA-3'-UTR interactions can be confirmed experimentally (39–42), these bioinformatic observations strongly suggested that a complex regulatory network between miRNAs and members of the FA/HR pathway exists.

In view of these high numbers of putative FA/HR-regulating miRNAs and based on the hypothesis that a defect in the FA pathway could be associated with attempts of the deficient cells to upregulate miRNA-controlled FA genes, we devised a functional screening approach to identify differentially expressed miRNA candidates by employing isogenic FA fibroblast cell line pairs with defects in *FANCA*, *FANCB*, *FANCC*, *FANCI* and *FANCJ*, respectively (Supplementary Material, Table S2). These cells were either complemented with oncoretroviral vectors expressing the cDNAs for the missing FA gene or were transduced with the corresponding control vectors with the same selection cassettes, as described elsewhere (43–49). First, we validated that cells deficient for *FANCA, -B, -C* and *-I* displayed only non-ubiquitinated FANCD2 protein, whereas their cDNA-corrected counterparts had largely monoubiquitinated FANCD2 upon induction of replication stress by hydroxyurea (Fig. 2). Further, consistent with a previous report, deficiency for FANCI led to an apparent instability of the FANCD2 protein (46). While FANCD2 monoubiquitination occurred normally in the deficient FA-*J* cells, as expected, high levels of the FANCJ protein were expressed in complemented FA-*J* cells but not their uncorrected counterparts (Fig. 2).

The miRNA expression profiles for the isogenic cell pairs were measured using the ABI TaqMan Assay, covering the most commonly expressed 377 miRNAs (pool A) (39). We then filtered the differentially expressed miRNAs in proficient versus deficient cells, based on a 2^{-ddCt} value (fold change) $\geqq 2$ (upregulation in corrected cells) and $\leqq 0.5$ (downregulation in corrected cells) (Fig. 3). The full miRNA expression profiles for each cell line pair are given in Supplementary Material, Table S3. In all analyzed cell line pairs, the number of miRNAs upregulated in proficient cells exceeded the number of miRNAs downregulated in proficient cells (Fig. 3). Twenty-seven miRNAs appeared upregulated in repair-proficient cells of at least two cell pairs, whereas only three miRNAs were downregulated in repair-proficient cells of at least two cell pairs (labeled in gray in Fig. 3). From these observations, we hypothesized that the preferentially decreased miRNA expression in deficient cells is related to the lack of FA/HR pathway functionality in these cells, resulting in their intention to upregulate miRNA-controlled FA/HR pathway members by decreasing expression of regulating miRNAs. Herein, miRNAs decreased in deficient cells from ≥ two cell pairs appear as the most promising candidates for functional relevance and subsequent analyses. Importantly, we did not find a correlation of the miRNAs downregulated in deficient cells and those miRNAs predicted to target the respective FA gene (data not shown).

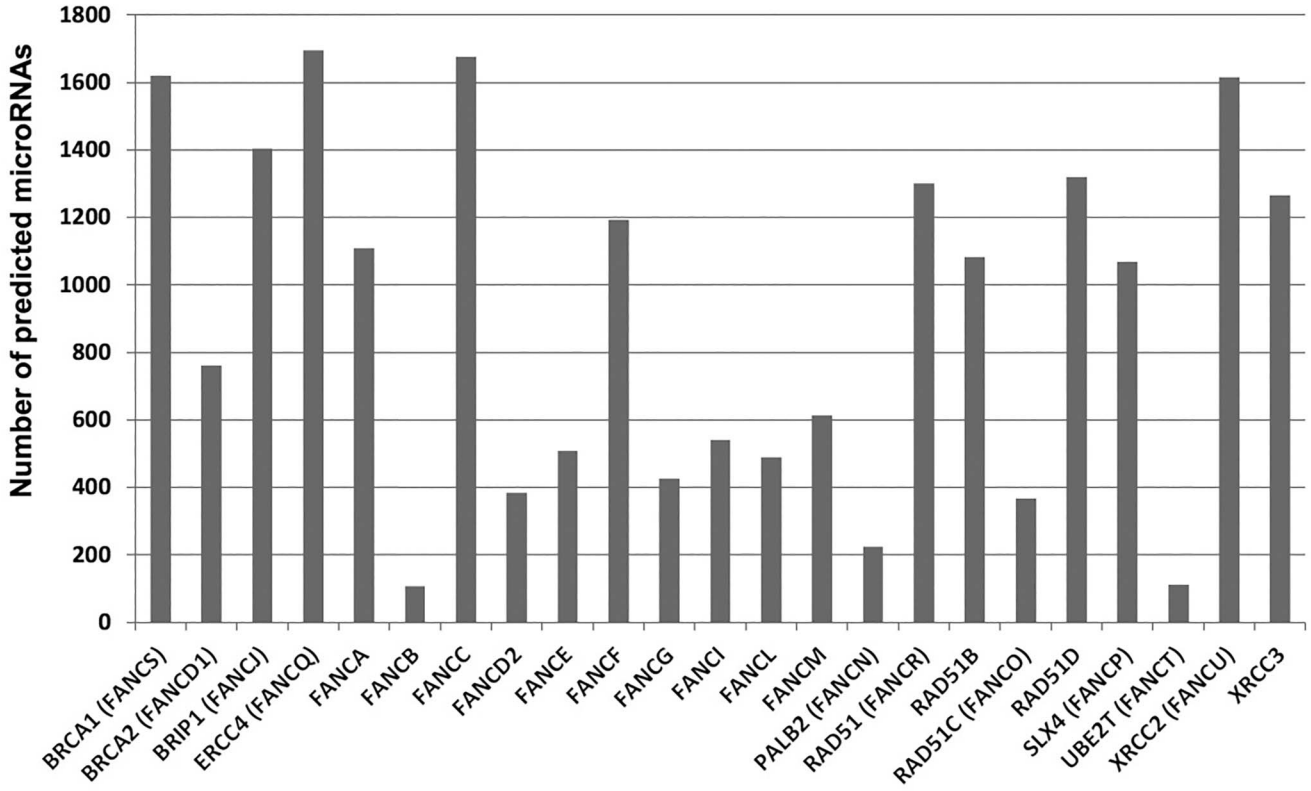

Figure 1. Summary of bioinformatically predicted miRNA regulation of FA/HR pathway members. To predict miRNAs that possibly regulate members of the FA/HR pathway, the bioinformatic miRNA target gene prediction webtool miRWalk 2.0 was employed for all 23 FA-related genes analyzed in this study, combining the results from embedded algorithms miRanda, PicTar2, TargetScan, miRDB, RNA22 and miRWalk. For each FA/HR pathway gene, the number of predicted regulatory miRNAs is plotted. Full target gene predictions are given in Supplementary Material, Table S1.

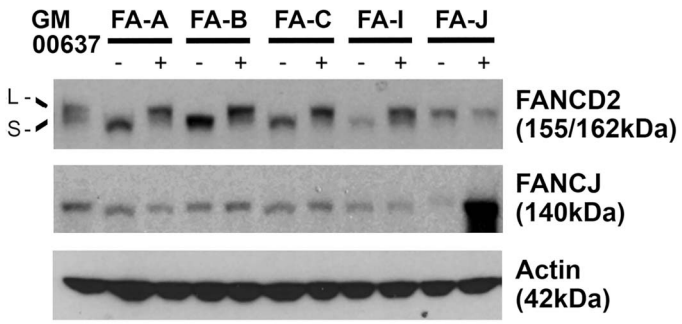

Figure 2. Correction of the FA-deficient cells by retroviral vectors. Monoubiquitinated FANCD2 protein (–L) was detected as a slower migrating band in immunoblots in corrected *FANCA*, *FANCB*, *FANCC* and *FANCI* cells but not in their deficient isogenic counterparts following treatment with 2 mM hydroxyurea for 16 h. The corrected cells also contained smaller amounts of non-ubiquitinated FANCD2 (-S). Normal FANCJ protein was detected in all cell lines, including the GM00637 SV40 transformed normal skin fibroblast line and their corrected counterparts.

Identification and validation of miRNAs regulating RAD51 paralogs in reporter gene assays and by western blotting

The bioinformatic analysis of our differential expression data revealed that 18 out of 27 miRNAs that were decreased in deficient cells from ≥ two cell line pairs were predicted to affect at least three of the six members of the *RAD51* gene family (Supplementary Material, Table S1). These findings match the observation that five out of six members of the RAD51 family (RAD51, RAD51B, RAD51D, XRCC2 and XRCC3) were consistently predicted to be regulated by ≥1000 miRNAs (Fig. 1). Compared to the remaining FA/HR genes analyzed, *RAD51* and its paralogs (including *RAD51C*) also show disproportionally high numbers of miRNA predictions relative to the lengths of their 3'-UTRs (Supplementary Material, Table S1). It should be noted here that three of the six RAD51 family members (*RAD51*, *RAD51C* and *XRCC2*) are also labeled FA genes (Fig. 1) (50,51). We therefore decided to focus our functional validation in cells on the RAD51 protein family and selected 11 miRNAs (miR-615-5p, miR-27b-3p, miR-98-5p, miR-130a-3p, miR-544a, miR-141-3p, miR-369-3p, miR-503-5p, miR-15a-5p and miR-494-3p) for these analyses, each predicted to regulate ≥3 RAD51 paralogs. Additionally, we included the miR-146a-5p, which was predicted to regulate only two RAD51 paralogs: RAD51D and XRCC3.

For experimental validation, we cloned the 3'-UTRs of *RAD51*, *RAD51B*, *RAD51C*, *RAD51D*, *XRCC2* and *XRCC3* behind the *firefly luciferase* ORF of the dual-luciferase (*firefly/renilla*) reporter vector pmirGLO and then analyzed the predicted 37 miRNA-3'-UTR

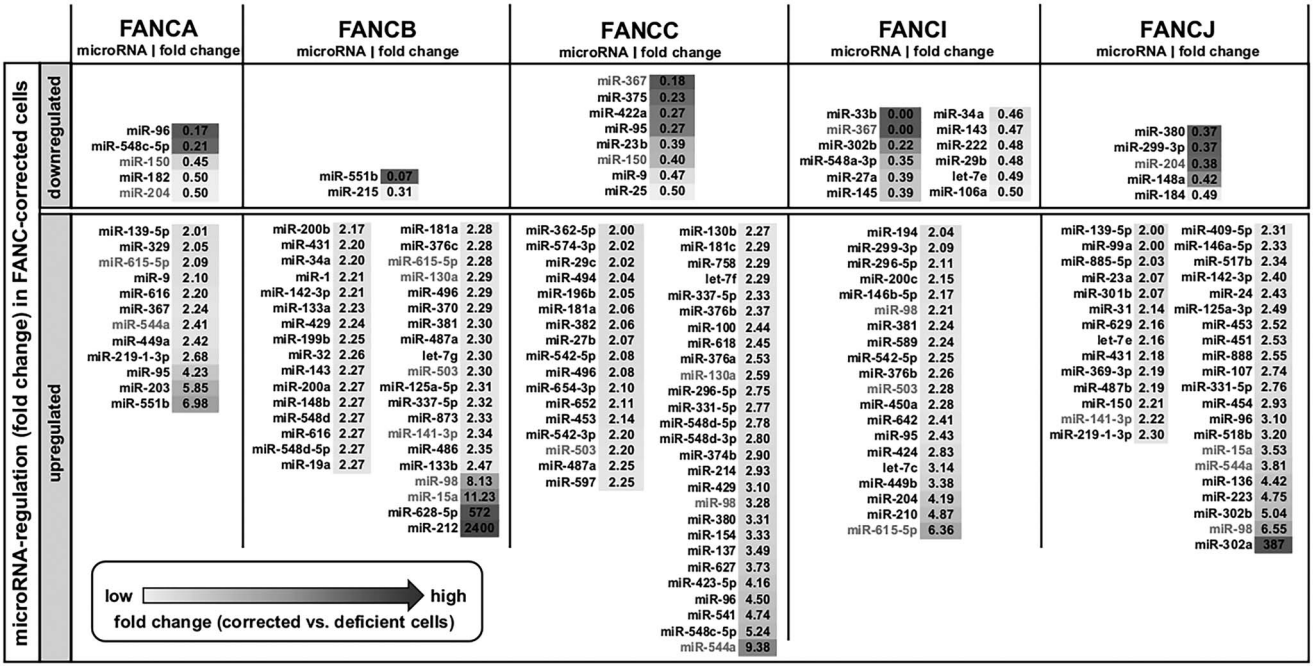

Figure 3. Differential miRNA expression in isogeneic cell pairs. Five isogeneic cell pairs, each deficient and corrected for the respective FA-gene (FANCA, FANCB, FANCC, FANCI, FANCJ), were comparatively analyzed for miRNA expression by qRT-PCR. MiRNAs differentially expressed by a fold change (2^{-ddCt}) ≥ 2.0 or ≤ 0.5 in corrected versus deficient cells from each pair are shown. The upper box shows miRNAs downregulated in corrected cells, whereas the lower box depicts miRNAs upregulated in corrected cells. Gray scales represent the degree of the fold change: light gray, low fold change; dark grey, high fold change. MiRNAs differentially expressed in at least two cell pairs are denoted in gray. In all cell pairs, the number of upregulated miRNAs in corrected versus deficient cells exceeded the number of downregulated miRNAs in corrected versus deficient cells, thus leading to a preferential lower miRNA expression in deficient cells of each isogeneic cell pair. Full miRNA expression data are given in Supplementary Material, Table S3.

interactions as described previously (39). Unexpectedly, the pmirGLO/XRCC2 3'-UTR construct gave unusual and non-reproducible results in the *firefly* luciferase activity measurements (data not shown) and thus had to be omitted from subsequent analyses. From the remaining 28 predicted interactions, miR-15a-5p, miR-494-3p and miR-544a functionally regulated RAD51D and miR-141-3p, and miR-369-3p regulated RAD51B (Fig. 4). Detailed results of the experimental target validations are given in Supplementary Materials, Figure S1.

We next determined the direct effects of miR-15a-5p, miR-494-3p and miR-544a on the abundance of RAD51D by western blotting analysis. The predicted binding sites for miR-15a-5p, miR-494-3p and miR-544a are spatially separate from each other on the 3'-UTR of RAD51D (Fig. 5A). Interestingly, in contrast to a control RAD51D siRNA, transfection of HEK293T cells with just one of these three miRNAs alone was not sufficient to reduce RAD51D protein level (Fig. 5B). However, transfection with an equimolar mixture of miR-15a-5p, miR-494-3p and miR-544a-mimics resulted in a significant reduction of the RAD51D protein to approximately 60% compared to the 100% mock control (Fig. 5C and D). We were unable to detect any effect of using miR-141-3p and miR-369-3p singly or in combination on RAD51B protein (data not shown) and thus omitted these miRNAs from subsequent experiments.

Gene ontology analyses suggest a broad influence of the three RAD51D-regulating miRNAs on DNA repair pathways

Although initially identified as RAD51D regulators, miR-15a-5p, miR-494-3p and miR-544a were also predicted to regulate additional members of the FA/HR pathway in humans (Supplementary Material, Table S1). Therefore, to investigate whether these miRNAs might exert a more widespread influence on DNA repair, we performed individual DNA repair-biased bioinformatic target gene prediction surveys for miR-15a-5p, miR-494-3p and miR-544a using miRWalk 2.0 under the aforementioned conditions. The predicted targets for each miRNA (Supplementary Material, Tables S4–S6) were then filtered for genes jointly identified by at least three of the six algorithms used in miRWalk 2.0, thereby omitting 60–70% of the original predictions. These reduced target gene lists of the individual miRNAs were subsequently analyzed for *gene ontology biological process* (GOBP) terms (52) employing the DAVID database (53,54) and then filtered for the key phrases *DNA damage*, *repair* and *recombination*, leading to 88 GOBP terms (Supplementary Materials, Tables S4–S6). In order to estimate the effects of miR-15a-5p, miR-494-3p and miR-544a expression on all *Homo sapiens* genes represented by the 88 GOBP terms related to the mentioned key phrases, we calculated the percentages of the putative target genes for each miRNA from the total numbers of *Homo sapiens* genes belonging to each particular GOBP term (as found at www.geneontology.org at the time of analysis) and plotted the results in Figure 6. The RAD51D-regulating miRNAs were predicted to regulate an average of 2–8% of the human genes assigned to each DNA repair-related GOBP term, often independently from the total number of genes belonging to the particular term. Strikingly, between 8.7% and 15.5% of the 103 human genes of the GOBP term '*double-strand break repair via homologous recombination*' were predicted targets of the three miRNAs, with miR-494-3p having the strongest putative impact (16 out of 103), followed by miR-15a-5p and miR-544a (Fig. 6). Cumulating the predicted targets of all three miRNAs that cover the GOBP term '*double-strand break repair via homologous recombination*', nearly 21% (22 out of 103) of the members of this GOBP term could possibly be affected by these miRNAs. It was thus highly likely that the impact of

Analyzed microRNAs			Target gene validations [Δ%]					
microRNA	Number of predicted FA-related genes	Differential expression in FA cell pairs	RAD51	RAD51B	RAD51C	RAD51D	XRCC2	XRCC3
miR-615-5p	*16*	A, B, I	-16		-22	-7	n/a	-22
miR-27b-3p	*14*	B, C		-17	-10	-1	n/a	2
miR-98-5p	*12*	B, C, I, J			-22	-17	n/a	
miR-130a-3p	*12*	B, C	11			-9	n/a	
miR-544a	*9*	A, C, J	4			29	n/a	3
miR-141-3p	*9*	B, J		27		-7	n/a	
miR-146a-5p	*9*	J				-13		12
miR-369-3p	*9*	J	10	23			n/a	
miR-503-5p	*8*	B, C, I	-8			5	n/a	
miR-15a-5p	*7*	B, J	11	15		36		
miR-494-3p	*7*	C	2			26	n/a	

<Δ5%	<Δ20%	<Δ30%	<Δ70%

Figure 4. Summary of experimental microRNA target gene validations on RAD51-paralogs. This crosstable summarizes target validation results of miRNAs miR-615-5p, −27b-3p, −98-5p, −130a-3p, −544a, −141-3p, −146a-5p, −369-3p, −503-5p, −15a-5p and − 494-3p on the 3′-UTRs of RAD51, RAD51B, RAD51C, RAD51D and XRCC3. The total number of predicted FA target genes for each miRNA is given in the second column; the third column denotes the FA cell pairs in which the respective miRNAs are differentially expressed (downregulated in deficient cells of FANC-A, -B, -C, -I or -J cell pairs). For each individual interaction of a particular miRNA and a RAD51-paralog 3′-UTR tested, the percental reductions of normalized Firefly activities from pmirGLO-3′-UTR + miRNA-mimic cotransfections, compared to pmirGLO + miRNA-mimic cotransfections, are given in the squares. These numbers are proportional to the effect of the respective miRNA on the individual 3′-UTR. The gray scale is depicted below the table: white, lacking microRNA effects; light gray, weak but significant ($P < 0.05$) miRNA effects; medium gray, moderate and significant ($P < 0.001$) microRNA effects; dark gray, strong and significant ($P < 0.001$) miRNA effects; n/a, not analyzed; empty squares, no particular prediction existent. Among 28 individual miRNA-3′-UTR interactions analyzed, miR-15a-5p, miR-494-3p and miR-544a were identified as regulators of RAD51D and miR-141-3p and miR-369-3p were found to regulate RAD51B. An additional five miRNAs showed weak interactions with their respective 3′-UTR counterparts (light gray squares). Note that XRCC2 could not be analyzed due to technical reasons. Detailed validation data which also include the n.t.siRNA specificity control are given in Supplementary Materials, Figure S1.

miR-15a-5p, miR-494-3p and miR-544a goes far beyond direct RAD51D regulation and also includes other members throughout the FA/HR pathway.

MiR-15a-5p and miR-494-3p regulate additional DNA repair genes

To investigate the regulatory potential of miR-15a-5p, miR-494-3p and miR-544a on the FA/HR pathway beyond RAD51D, we experimentally tested predictions of genes from the FA/HR pathway (*BRCA1*, *FANCA*, *FANCF*, *FANCG*, *FANCJ*, *FANCM*) as well as additional predictions from the GO term '*double-strand break repair via homologous recombination*' (*MMS22L*, *EXD2*, *RNF138*). As demonstrated in Figure 7A, *FANCG*, *MMS22L* and *EXD2* emerged as true targets of miR-494-3p and *FANCA* as well as *FANCM* were regulated by miR-15a-5p. Among the tested candidates, no target gene was identified for miR-544a. The strong regulatory potential of miR-15a-5p, miR-494-3p and miR-544a is visualized by the virtual interaction network (Fig. 7B) consisted of validated and putative interactions with members from the GO term '*double-strand break repair via homologous recombination*'.

RAD51D-regulating miRNAs influence RAD51 foci formation

RAD51 is the central recombinase in eukaryotes that catalyzes the transfer between a broken DNA sequence and the undamaged strand homologue, thereby inducing re-synthesis of the damaged DNA region (10,13,15). Importantly, as deficiency of any of the RAD51 paralogs and numerous other FA/HR genes will influence or even abrogate RAD51 foci formation upon irradiation/DNA damage, RAD51 foci analysis is a sensitive marker for the recombination process (10,13,15). Therefore, given their role in regulating RAD51D, in order to test the functional impact of miR-15a-5p, miR-494-3p and miR-544a expression on RAD51 foci formation, U2OS cells were transfected with (i) an equimolar mixture of miR-15a-5p, miR-494-3p and miR-544a mimics, (ii) each of these mimics separately, (iii) a RAD51D specific siRNA or (iv) an unspecific non-targeting siRNA (n.t.siRNA) and then analyzed for RAD51 foci formation as described previously (21). Transfection of U2OS cells with the miRNA mixture resulted in a strong inhibition (approximately 70%) of foci formation when compared to mock- and n.t.siRNA-transfected control cells (Fig. 8). The inhibition by the miRNA mixture was even stronger than the one induced by RAD51D siRNA. Interestingly, transfections with the single miRNA mimics revealed that the effect of the miRNA mixture was solely caused by miR-494-3p and neither miR-15a-5p nor miR-544a significantly contributed to the inhibition of RAD51 foci formation (Fig. 8B).

Expression of RAD51D-regulating miRNAs inhibits HR

Finally, to analyze the influence of miR-15a-5p, miR-494-3p and miR-544a expression on the function of the entire FA/HR pathway, we employed the well-established U2OS-DR cells (55,56), which contain two inactive GFP fragments, *SceGFP* and *iGFP*, the former bearing a recognition site for endonuclease *I-SceI*. Upon induction of a site-specific DNA DSB by expression of *I-SceI* in the cells, the repair of a functional *GFP* cDNA by HR occurs and can be semiquantified by flow cytometry analysis.

Cotransfection of the single miRNAs and the I-SceI-GR-RFP plasmid revealed that miR-494-3p exhibits the strongest

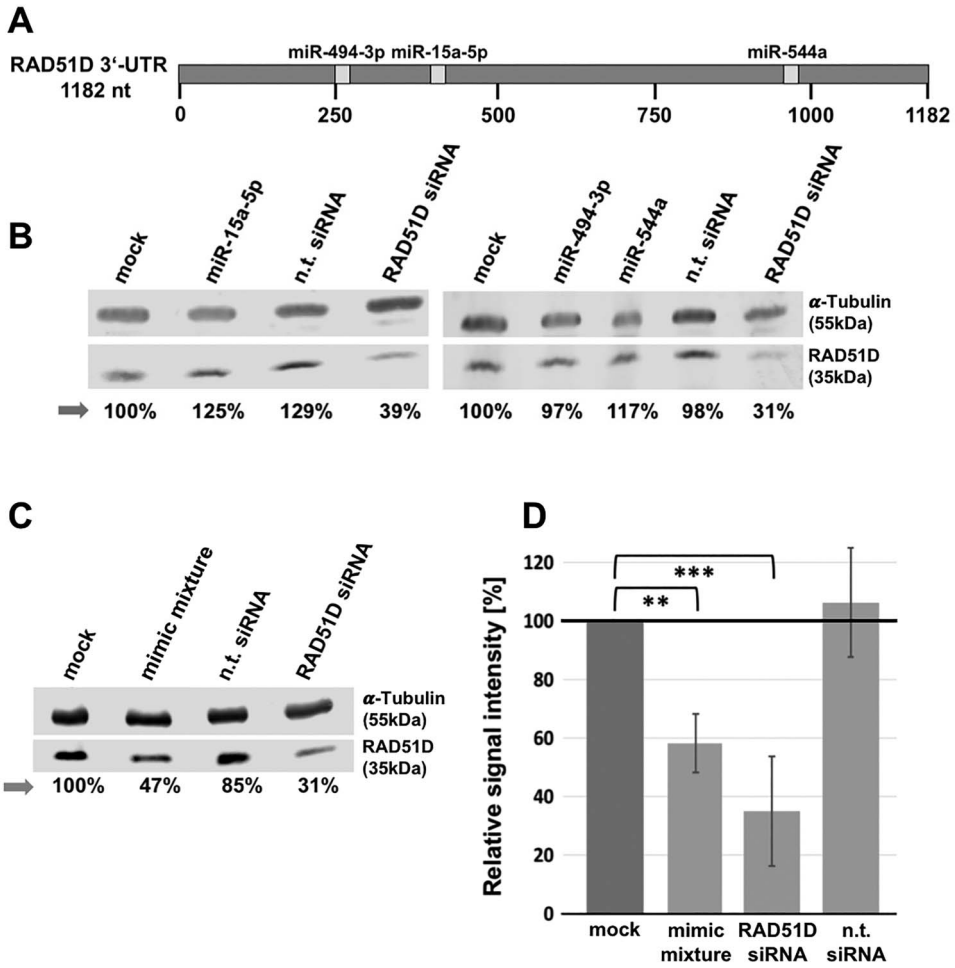

Figure 5. Effects of miRNAs on expression of the RAD51D protein. Cells were transfected with the appropriate miRNA mimics, RAD51D siRNA or n.t.siRNA, and protein abundance changes were analyzed by western blotting. Arrows point to the normalized percentages compared to reference values (100%) from mock-transfected cells. (A) Distribution of predicted miRNA binding sites on the RAD51D-3'-UTR. The distances between the individual binding sites allow for parallel binding of miR-15a-5p, miR-494-3p and miR-544a. (B) Single transfections of HEK293T cells with miRNA-mimics miR-15a-5p, miR-494-3p or miR-544a resulted in no significant effect on RAD51D protein abundance. (C) Transfection of HEK293T cells with an equimolar mixture of miRNA-mimics miR-15a-5p, miR-494-3p and miR-544a resulted in a downregulation of RAD51D protein. However, the RAD51D siRNA showed even stronger effects. (D) Summary of three independent western blot replicates using the mimic mixture confirms a significant (Student's *t*-test, unpaired, ** $P \leq 0.01$, *** $P \leq 0.001$) downregulation of RAD51D protein upon transfection with the mimic mixture.

influence on the HR efficiency by significantly reducing the amount of GFP$^+$ cells to approximately 25% (Fig. 9) when compared to cells transfected with the I-SceI-GR-RFP plasmid only (mock). Reduction was also significant when compared to RAD51D siRNA-transfected cells. Expression of miR-15a-5p showed a slightly weaker influence on HR, reducing the amount of GFP+ cells to approximately 40%, whereas miR-544a exhibited only moderate, non-significant effects on the repair of GFP (Fig. 9). Cotransfection of an equimolar mixture of miR-15a-5p, miR-494-3p and miR-544a together with ISceI-GR-RFP resulted in an even stronger and highly specific decrease of HR, significantly reducing the amount of GFP$^+$ cells to nearly 10% compared to mock-transfected or negative controls (Fig. 10). This reduction by far exceeded the impact of the most effective miRNA miR-494-3p (Fig. 9B), while the RAD51D-specific siRNA only weakly reduced HR in both experiments. These results suggest that miR-494-3p and miR-15a-5p have targets in the FA/HR pathway beyond RAD51D.

Discussion

The latest miRBase release (http://www.mirbase.org/, release 22.1, October 2018) lists 2693 mature human miRNAs originating from 1984 precursor molecules. Our initial bioinformatics prediction that 107 of 1696 miRNAs putatively regulate each one of the analyzed FA/FA-associated genes points to a huge, however, experimentally largely undefined functional miRNA network, which possibly fine-tunes the expression of these FA/HR genes. However, since usually only a minority of the predicted miRNAs actually serve as real *in vivo* regulators (39–42), it is an important task in the field to identify and select promising miRNA candidates for subsequent functional studies. To this end, we hypothesized that loss- and gain-of-FA-function in isogeneic cell pairs might be reflected in differentially miRNA expression, thereby possibly pointing to miRNAs functionally involved in the regulation of the FA/HR pathways. For this screen, we selected five FA genes, not known to be regulated by miRNAs at the initiation of these

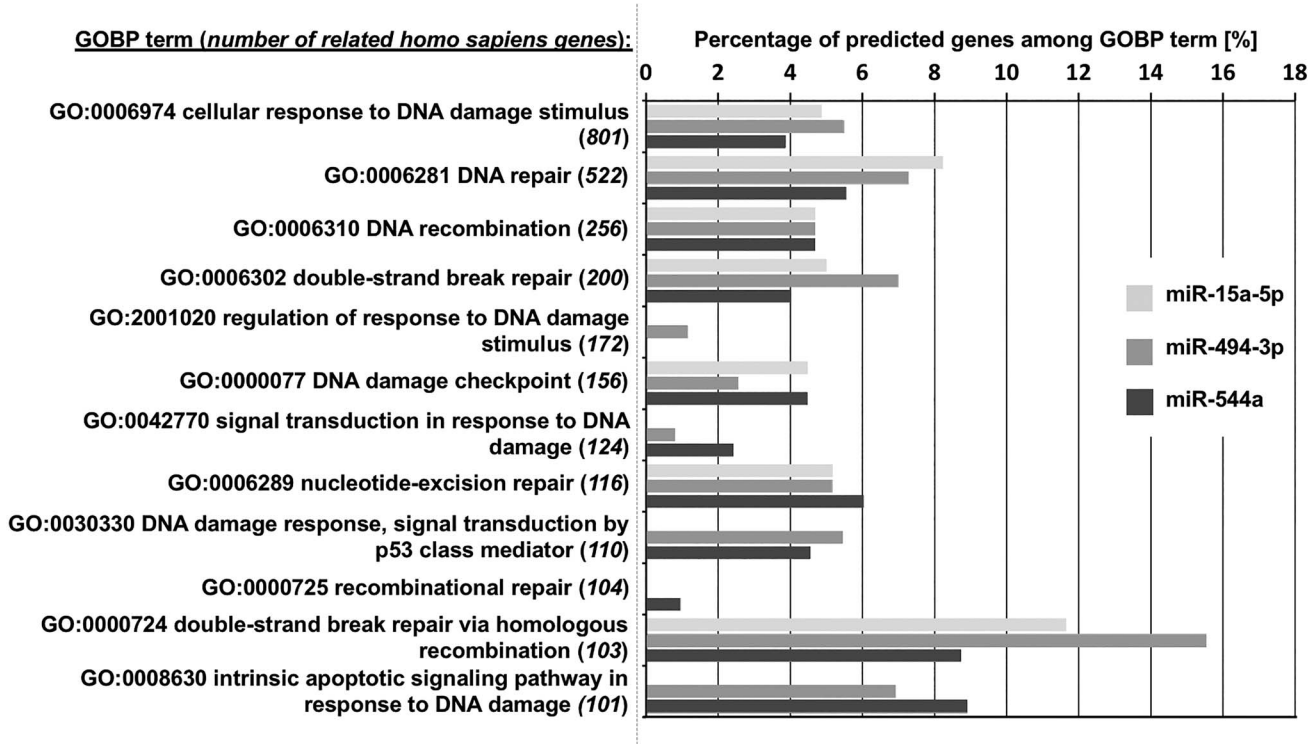

Figure 6. Gene ontology analysis. Target genes of miR-15a-5p, miR-494-3p and miR-544a which had been predicted by ≥3 algorithms in parallel by miRWalk 2.0 were analyzed for their representation among members of GOBP terms related to keywords *recombination*, *repair* and *DNA damage*. The percental representation of predicted targets among the total number of human genes filed under a given GOBP term (shown in brackets behind the respective term) in the *gene ontology* database is plotted. The figure is limited to GOBP terms represented by > 100 human genes. In general, approximately 2–8% of the genes filed under a particular GOBP term, as shown here, are predicted targets for the three miRNAs. However, members of the GOPB term *GO: 0000724 double-strand break repair via homologous recombination* are clearly overrepresented in this analysis, especially the putative targets of miR-494-3p and miR-15a-5p, which represent nearly 16% and 12% of the total genes of this GOBP term, respectively. Detailed information on this analysis is given in Supplementary Materials, Tables S4–S6.

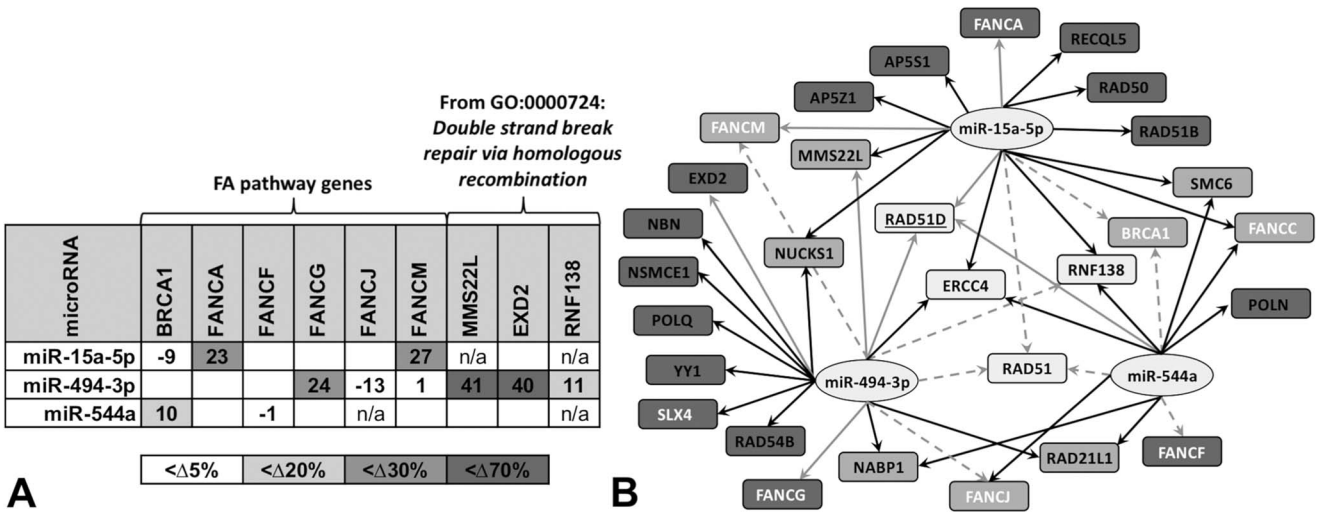

Figure 7. Complementing experimental microRNA target gene validations and virtual interaction network. (**A**) MiRNAs miR-15a-5p, miR-494-3p and miR-544a were tested with 3′-UTRs from selected members of the FA pathway and members of the GOBP term *GO: 0000724 double-strand break repair via homologous recombination*. Validations were performed and are presented as described in Figure 4. MMS22L, EXD2 as well as FANCG were identified as miR-494-3p targets; FANCA and FANCM were shown to be regulated by miR-15a-5p. n/a: not analyzed. (**B**) Virtual Network of regulatory interactions between miR-15a-5p, miR-494-3p and miR-544a (ovals) and their predicted target proteins from the GOBP term "*double-strand break repair via homologous recombination*" (gray rectangles, black lettering) and from members of the FA pathway (gray rectangles, white lettering). Dark gray rectangles: targets predicted by one miRNA; medium gray rectangles, targets predicted by two miRNAs; light gray rectangles, targets predicted by three miRNAs. RAD51D, which originally identified miR-15a-5p, miR-494-3p and miR-544a as regulating miRNAs, is underlined. Arrows denote miRNA–target gene interactions: black arrows, predicted miRNA–target interaction; gray arrows, predicted interactions verified by reporter assays (Figs 4 and 7A); dashed gray arrows, predicted interactions falsified by reporter assays.

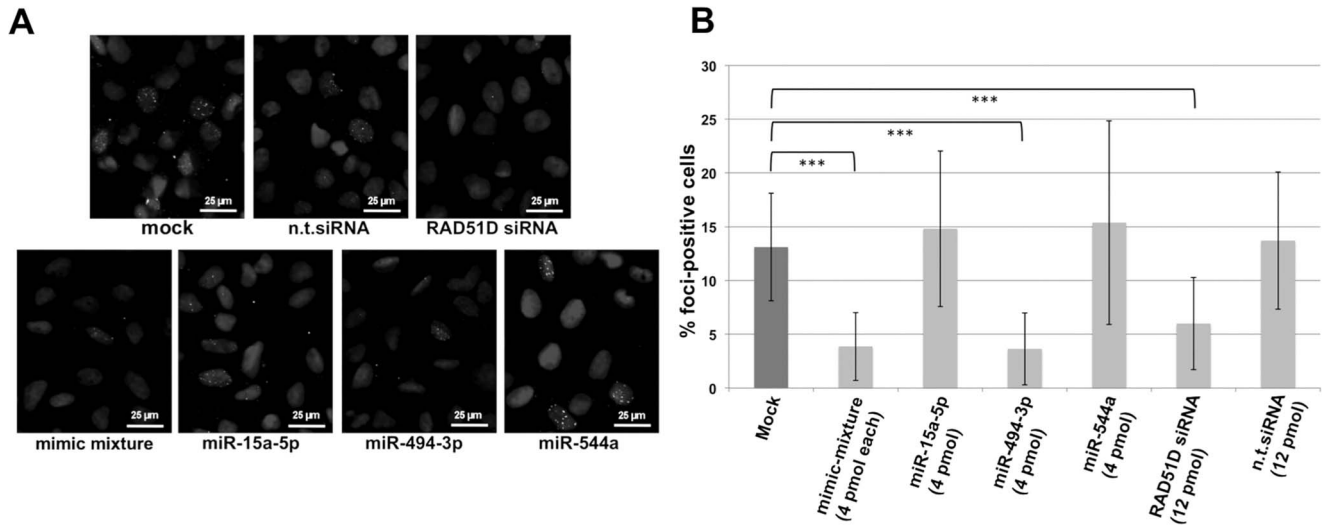

Figure 8. RAD51 foci analysis. U2OS cells were transfected with an equimolar mixture of miR-15-5p, miR-494-3p and miR-544a mimics (mimic-mixture), each miRNA-mimic alone, or controls (RAD51D siRNA and n.t.siRNA), irradiated with 10 Gray 48 h post transfection and analyzed for RAD51 foci 6 h after irradiation. (**A**) Representative photographs of RAD51/DAPI stainings for each transfection condition (scale bar: 25 μm). Images are magnified picture sections from the respective full photographs. (**B**) Results from two biological transfection replicates, with overall 700–1000 cells (from approximately 10 photographs/transfection condition) counted for each transfection condition, together with statistical significances (Student's *t*-test, $^{***}P > 0.001$). Transfection with the equimolar miRNA-mixture as well as with miR-494-3p and RAD51D siRNA led to a strong and highly significant reduction of visible RAD51 foci. Transfections with miR-15a-5p or miR-544a did not affect RAD51 foci. Note that fluorescence signals from outside the DAPI-stained nuclei were not counted.

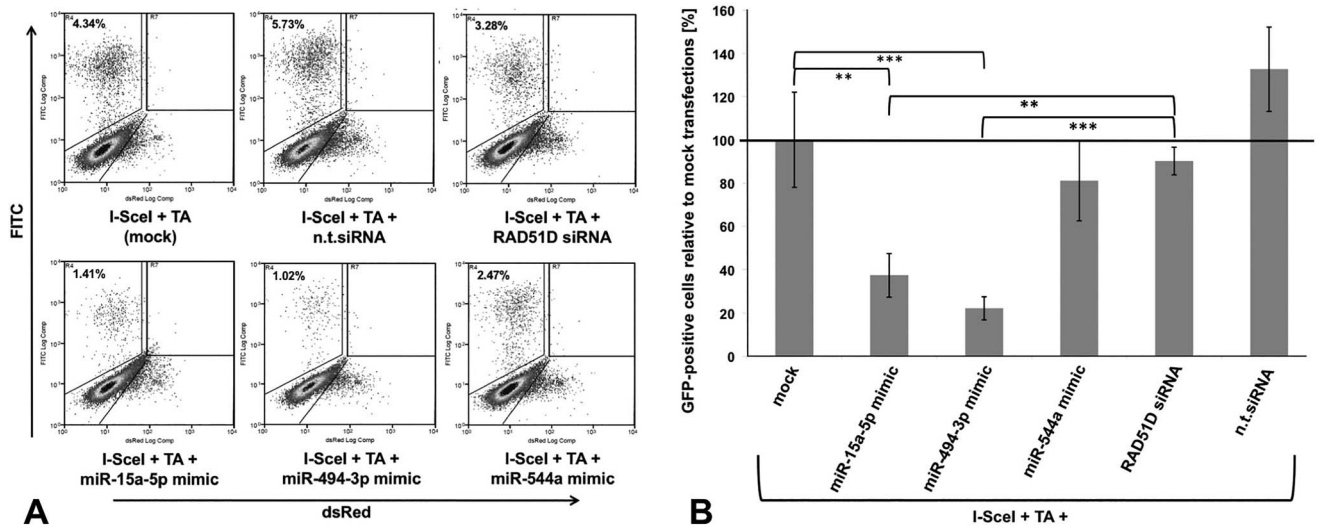

Figure 9. Inhibition of homologous recombination by miR-15-5p, miR-494-3p and miR-544a. U2OS cells were cotransfected with ISceI-GR-RFP vector together with one of the appropriate microRNA mimics, RAD51D siRNA (positive control), n.t.siRNA (negative control) or no additional small RNA (vector-only, mock). Nuclear ISceI import was induced by addition of TA 48 h post transfection, and cells were analyzed by flow cytometry 48 h after induction and gated for the GFP-positive population. (**A**) Representative FACS analyses of GFP repair upon transfections of miRNAs miR-15a-5p, miR-494-3p or miR-544a. (**B**) Summary of four independent replicates of single transfections using miRNAs miR-15a-5p, miR-494-3p or miR-544a in comparison to mock-transfected cells. Mean values of GFP-positive cell numbers are given in percent compared to the mock control (100%), together with statistical significances (mock versus miRNA mimics and RAD51D siRNA versus miRNA mimics; Student's t-test, $^{**}P < 0.01$, $^{***}P < 0.001$). MiR-15a-5p and miR-494-3p significantly reduced GFP-repair compared to mock- and RAD51D siRNA-transfected cells, whereas both miR-544a and RAD51D siRNA showed only weak non-significant effects compared to mock-transfected cells.

studies (57): *FANCA* and *FANCC* are the two most frequent FA genes worldwide and *FANCB* is the only gene located on the X-chromosome (58). These three FA genes function early in the FA/HR pathway, prior to the monoubiquitination and phosphorylation of the FANCD2/FANCI protein dimer, which itself is needed for stabilization of the stalled replication fork at the crosslink (58). From this dimer, we choose *FANCI*. *FANCJ/BRIP1* was included in the initial screen as a late FA gene, acting downstream of FANCI and FANCD2 monoubiquitination (10). Importantly, we validated deficiency and proficiency for FANCA, -B, -C and -I in cell pairs based upon the absence or presence of monobubiquitination, and for FANCJ based upon the presence or absence of the protein that it encodes.

Using the TaqMan Megaplex qPCR assay to determine the expression of the 377 most commonly expressed miRNAs, our analysis revealed that the majority of miRNAs differentially expressed in the isogeneic cell pairs showed lower abundance in the respective FA-deficient cells and remarkably, only a

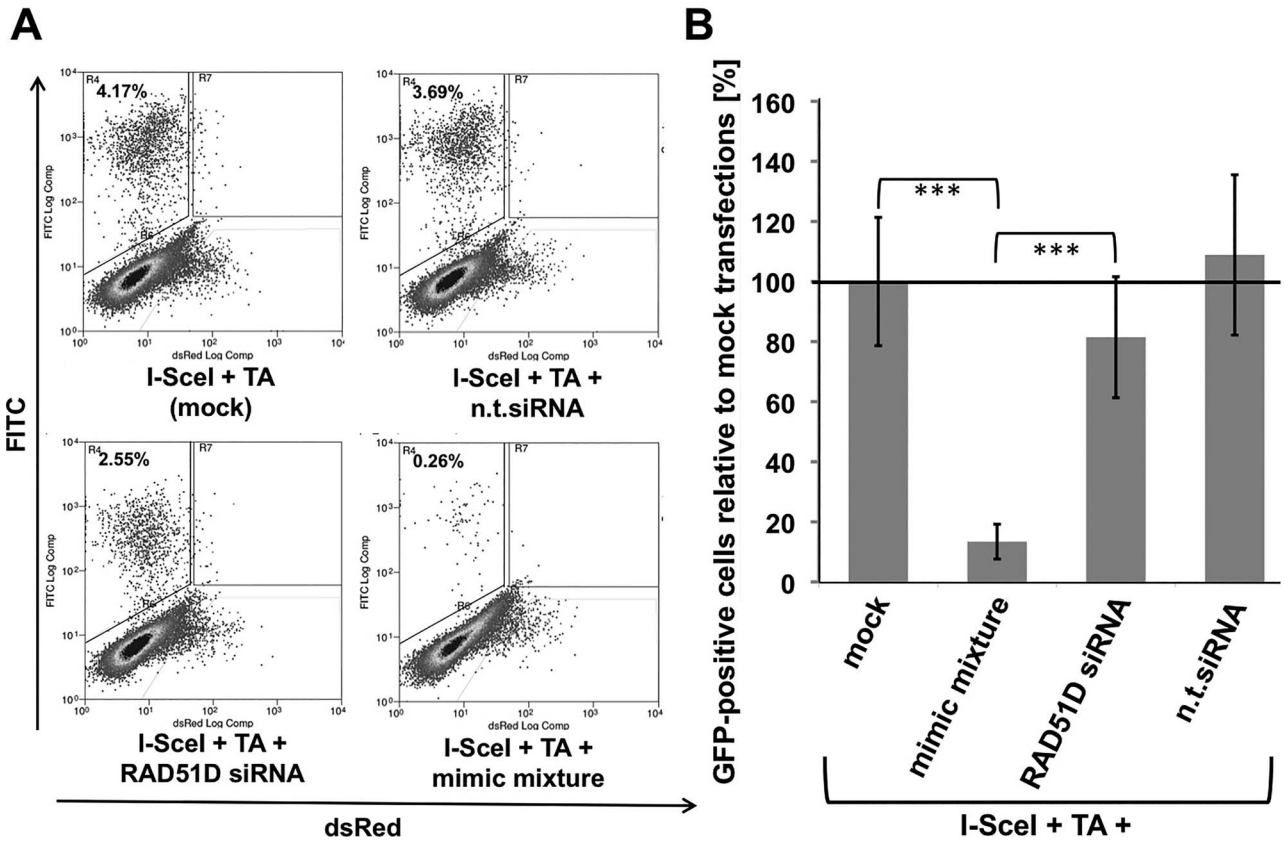

Figure 10. Inhibition of homologous recombination using a mixture of miR-15a-5p, miR-494-3p and miR-544a mimics. Analyses were performed as described in Figure 9. (**A**) Representative FACS analyses of GFP repair upon transfection of an equimolar mixture of miR-15a-5p, miR-494-3p and miR-544a. (**B**) Summary of FACS analyses of four independent replicates of miRNA mixture transfections. Transfection of the miRNA mixture resulted in a strong and highly significant inhibition of HR compared to mock- as well as RAD51D siRNA-transfected cells (Student's t-test, $***P < 0.001$). This reduction exceeded the effect of any of the single miRNAs tested (Fig. 9).

minority of miRNAs was expressed in a reciprocal pattern. This preferentially lower miRNA expression in FA-deficient cells seems to reflect the effort of the deficient cells to regain functionality by stronger expression of FA/HR-associated miRNA-target genes via downregulation of regulatory miRNAs.

Combined with bioinformatic analyses, our screen prominently pointed to miRNAs putatively regulating RAD51 paralogs. After removal of XRCC2, 10 of the remaining 28 putative individual miRNA–RAD51 paralog interactions were predicted as candidates by at least three out of six independent algorithms used and five of these were confirmed in reporter gene assays to regulate RAD51B or RAD51D translation. However, none of the seven miRNAs from our screen that were predicted to regulate *RAD51* appeared to be true inhibitors of this gene. This finding contrasts with the description of RAD51 as one of the most intensively miRNA-controlled factors in HR (57). For example, members of the miR-34-familiy suppress RAD51 and decrease HR repair efficiency (30,59). RAD51 is also regulated by miRNAs miR-143b* and miR-193b* (60), miR-96 (28) and miR-506 (61). In comparison, very little is known about miRNA regulation of the RAD51 paralogs: RAD51C was described as a regulatory target of miR-222 (62) and miR-3940-5p downregulates XRCC2 and thereby affects RAD51 foci formation (63).

It is important to realize that, despite the results from the initial reporter assays, transfection of an equimolar mixture of miR-15a-5p, miR-494-3p and miR-544a mimics was necessary to downregulate RAD51D protein in immunoblots, while using the individual miRNAs alone failed to influence RAD51D protein levels. However, since the predicted binding sites for these three miRNAs are located separately from each other on the 3'-UTR of RAD51D, it is a compelling hypothesis that miR-15a-5p, miR-494-3p and miR-544a function together in an additive or synergistic manner to inhibit RAD51D translation. Reporter gene-based experimental target validations do not necessarily reflect the real miRNA-mediated target protein regulation *in vivo* (41,64) and indeed, miRNAs miR-141-3p and miR-369-3p failed to reduce RAD51B protein levels in immunoblots at all, even when applied as an equimolar mixture (data not shown).

Despite the rather weak effects of miR-15a-5p, miR-494-3p or miR-544a on RAD51D protein levels, the *gene ontology* analyses strongly suggested an especially robust effect of these miRNAs on HR in general, due to the striking overrepresentation of their predicted target genes in the GOBP term '*double-strand break repair via homologous recombination*', especially with regard to miR-494-3p. This notion was supported experimentally by identifying *MMS22L, EXD2, FANCA, FANCM* as well as *FANCG* as additional regulatory targets of miR-15a-5p or miR-494-3p, thus supporting broad regulatory roles of at least miR-15a-5p and miR-494-3p on DNA repair genes in the FA/HR pathways.

As the ultimate proof for the effects of miR-15a-5p, miR-494-3p and miR-544a on HR *in vivo* in cells, we used RAD51 foci formation and HR-mediated GFP damage repair as two widely accepted standard functional assays for HR (21,55,56,65,66). Formation of RAD51 foci on protruding single strands as the central step during HR is dependent on the RAD51D-containing BCDX2 complex (67). Strikingly, while the mixture of all three miRNAs was necessary

to reduce RAD51D protein level in western blotting, miR-494-3p by itself was already sufficient for reduction of RAD51 foci formation with no further contributions coming from miR-15a-5p and miR-544a. As miR-494-3p notably failed to directly regulate RAD51 in our target validations, these results suggest that miR-494-3p affects RAD51 foci formation not only by reducing RAD51D, but also through regulation of additional targets involved in RAD51 foci formation (10). Two possible targets are MMS22L and EXD2, which were strongly regulated by miR-494-3p in the reporter gene assays performed. Mechanistically, MMS22L interacts with TONSL and is required for efficient RAD51 foci formation (68), whereas EXD2 is an interactor of the MRE11-RAD50-NBS1 (MRN) complex necessary for DNA end resection upstream of RAD51 foci formation (10). Importantly, MRE11A, RAD50 and NBS1 are also known targets of miR-494-3p (69) and EXO1, which mediates long-range end resection following the initial resection facilitated by the MRN complex (70,71), is among the predicted targets of miR-494-3p. Taken together, these observations strongly suggest that miR-494-3p exerts a multi-target based inhibition during the initial stages of HR and they can readily explain the strong regulatory effect of transient mir-494-3p transfection on RAD51 foci formation, despite its only weak effects on RAD51D.

In the HR-mediated GFP damage repair assay, the overexpression of both miR-494-3p and miR-15a-5p was associated with strong and significant reductions in the repair of damaged GFP when compared to mock-transfected U2OS-DR cells. MiR-15a-5p alone did not affect RAD51 foci formation and thus might regulate HR at later steps downstream of RAD51 foci formation. In summary, as miR-544a showed only weak effects on HR, remarkably, these results match the 'ranking' of the three miRNAs in the GOBP analyses. Further, the even stronger effect of a mixture of the three miRNAs on HR clearly suggests additive or synergistic effects on HR. Interestingly, the highly specific siRNA inhibition of RAD51D only slightly affected repair of GFP, despite its clear effects on RAD51D protein levels and RAD51 foci formation. However, as there is no clinical phenotype in humans with only one functional RAD51D germline allele (22) and approximately 35% of the RAD51D protein was still detectable using the siRNA, it appears highly likely that the weak impact of RAD51D siRNA transfection on HR is due to the residual RAD51D protein in the cells. To our knowledge, only one group described regulation of RAD51D by two miRNAs, miR-103 and miR-107, which are identical except for one base exchange at the second last base at their 3′-end (31). These two miRNAs also directly target RAD51 (31); hence, the reduction of the HR repair efficiency and the increased sensitivity to DNA damaging agents can occur through parallel downregulation of both RAD51 family members.

In addition to inhibiting the MRN complex, miR-494-3p can also exacerbate DNA damage and influence endothelial senescence (69), but so far has not been described to directly inhibit HR in cells. As several FA/HR pathway genes targeted by the three miRNAs are well-established cancer susceptibility genes, it is not surprising that miR-494-3p has been identified as a tumor-driving miRNA, which promotes lung carcinogenesis. Additionally, by modulating NOTCH1 and PTEN/PI3K/AKT signaling and CASP2-dependent apoptosis, miR-494-3p promotes migration of breast cancer cell lines (72–75). High miR-494-3p expression is also linked to poor survival in breast cancer patients (76) and overexpression of miR-494-3p is currently discussed as a prognostic tumor marker (77). The other two miRNAs, miR-15a-5p and miR-544a, have not yet been reported to be involved in DNA repair processes. However MiR-15a-5p is known as a tumor-suppressing miRNA by targeting MYCN and WNT3A (78,79), and miR-544a influences gastric cancer by regulating GKN1 (80) and also can induce epithelial-mesenchymal transition by activating WNT signaling pathways (81). Interestingly, miR-98-5p, which was highly abundant in the corrected cells in four out of five isogenic FA cell line pairs (Fig. 3), contributes to cisplatin resistance in epithelial ovarian cancer cells by regulating Dicer1 (82).

In conclusion, although originally identified by their regulatory impact on RAD51D, miR-15a-5p, miR-494-3p and miR-544a emerge in our study as miRNAs influencing the activity of the entire FA/HR pathway through multiple target gene interactions. Thus, our approach of using comparative miRNA expression analysis in isogenic DNA repair deficient and proficient cell pairs is a very feasible strategy to identify additional miRNAs important in the repair of defined DNA damage types. Ultimately, understanding and, subsequently, modulating miRNA-mediated regulation of essential DNA repair pathways in cells might also be beneficial for counteracting the lower repair capacity of patients with biallelic hypomorphic mutations, e.g. FA. Furthermore, understanding miRNA-mediated regulation of DNA repair genes might provide a basis for developing and engineering synthetic lethality strategies useful for patients with acquired or germ-line mutations in cancer-associated FA/HR genes.

Materials and Methods

Cell lines and culture

For the miRNA expression screen, we used isogenic human fibroblast cell line pairs, which were either defective for a particular FA gene or corrected for the genetic defect by using a retroviral expression cassette with a cDNA for the particular FA gene. Control cells contained the same retroviral vector with an IRES-neomycin resistance gene (neoR), however, lacked the corresponding FA cDNA. The isogeneic cell pairs with loss-of-functions of the following FA-genes (Supplementary Material, Table S2) were previously published: *FANCA* (43,44), *FANCB* (44,45), *FANCC* (44), *FANCI* (46,47) and *FANCJ* (48,49). GM00637 cells obtained from Coriell repositories were utilized as normal SV40 transformed skin fibroblast controls in western blot experiments with the above FA cell lines. Experimental target validations and RAD51D western blots were carried out in HEK293T cells. U2OS cells were used for RAD51B western blots, RAD51 foci assays and GFP-based recombination assays (55). FA cell lines and the GM00637 and HEK293T cells were cultured in DMEM, high glucose medium supplemented with fetal calf serum FCS (10%) and penicillin/streptomycin (1%). FA cells were grown under hypoxic conditions (6% O_2). U2OS-DR/GFP cells were cultured in McCoy's 5A medium supplemented with FCS (10%) and penicillin/streptomycin (1%) and incubated with puromycin (2 μg/mL) for selection purposes.

MiRNA expression analysis

Preparation of total RNA was performed using the Ambion *mir*Vana miRNA Isolation kit (Applied Biosystems, Darmstadt, Germany) according to the manufacturer's instructions, with the sole exception of direct lysis of adherent cells, thereby omitting trypsinization. Total RNA was used for miRNA expression analysis employing the TaqMan miRNA Megaplex array (pool A, Applied Biosystems) (83) according to the manufacturer's instructions. In brief, 350 ng RNA was reverse transcribed and pre-amplified for 12 PCR cycles, followed by TaqMan probe-based array amplification for 40 additional PCR cycles. Raw Ct-values were normalized to U6 RNA data and ddCt as well as $2^{-(ddCt)}$ data were calculated. Fold changes ($2^{-(ddCt)}$) of $\geqq 2$ or $\leqq 0{,}5$ were considered as differentially expressed, as previously described (39,40).

Bioinformatic analyses

Bioinformatic miRNA target gene predictions were performed using the webtool miRWalk 2.0 (33) (http://zmf.umm.uni-heidelberg.de/apps/zmf/mirwalk2/) combining the results from the implemented algorithms miRanda (34) (http://www.microRNA.org), miRDB (37) (http://www.mirdb.org), mirWalk (33), PICTAR2 (35), RNA22 (38) (https://cm.jefferson.edu/rna22) and Targetscan (36)(http://www.targetscan.org). For subsequent GO (52) analyses of predicted target genes, we employed the webtool DAVID (53,54)(https://david.ncifcrf.gov/content.jsp?file=fact.html) and the embedded *Gene Ontology* database (www.geneontology.org). To increase the reliability of the output, only target genes for a particular miRNA that were predicted by at least three of the aforementioned six prediction algorithms were used as input for the DAVID database.

Experimental miRNA target gene validation

PCR-generated full-length 3'-UTR fragments from RAD51 (NM_002875.4), RAD51B (NM_133509.3), RAD51C (NM_058216), RAD51D (NM_002878.3) and XRCC3 (NM_001100119) were cloned at the 3′-end of dual-luciferase (*firefly* and *renilla*) reporter vector pmirGLO (Promega, Mannheim, Germany). The 3'-UTR of XRCC2 (NM_005431) was cloned as fusion between a commercially synthesized fragment and a PCR product to generate the full-length 3'-UTR. All 3'-UTR constructs in pmirGLO were sequenced. Validations of predicted miRNA-3'-UTR interactions were carried out in HEK293T cells as described previously (39,40). To normalize for effects of endogenous HEK293T miRNAs, empty *firefly/renilla* dual reporter vector pmirGLO and respective pmirGLO/3'-UTR constructs were each transfected into HEK293T cells. *Firefly* and *renilla* activities were determined 24 h after transfection. Relative *firefly* activities from these transfections were used as references. Relative *firefly* activities were then compared with those of pairwise cotransfections of these vectors with the respective miRNA mimic (Dharmacon, Bonn, Germany) to test for unspecific effects of the given miRNA-mimic on *firefly/renilla* per se, as well as for its effect on the respective 3'-UTR. The specificity of interactions was tested by replacing the mimic by an unspecific non-targeting siRNA (n.t.siRNA). Percental reductions of normalized *firefly* activities from pmirGLO-3'-UTR + miRNA-mimic cotransfections compared to pmirGLO + miRNA-mimic cotransfections described the effect of the given miRNA on the particular 3'-UTR. All transfections were performed in at least two independent biological experiments with three to four technical replicates each.

Western blotting

HEK293T cells were grown in six-well plates to a density of 3×10^5 cells/well and transfected with 40 pmol/well of the appropriate miRNA mimic, a RAD51D specific siRNA or the unspecific n.t.siRNA, respectively, as described previously [35]. Briefly, proteins were isolated 48 h after transfection and approximately 80 μg of protein/lane were separated on denaturing polyacrylamide gels followed by blotting onto nitrocellulose membranes. The following primary antibodies were used in this study: rabbit RAD51D (Abcam, Berlin, Germany, ab202063), rabbit RAD51B (Thermo Fisher, Darmstadt, Germany, PA5–28351) and mouse anti-α-tubulin (Sigma Aldrich, Taufkirchen, Germany, T5168). Antibody signals were visualized using IRDye 680LT (anti-mouse) and IRDye 800CW (anti-rabbit, both: LI-COR Biosystems, Bad Homburg, Germany Biosystems) coupled secondary antibodies followed by scanning and quantification using the LI-COR infrared detection system and the Odyssey 2.1 software (LI-COR Biosystems, Bad Homburg, Germany). Quantified signals were normalized to housekeeping protein α-tubulin.

For western blots with uncorrected/corrected FA cell line pairs with germline deficiency for *FANCA*, *FANCB*, *FANCC*, *FANCI* and *FANCJ*, with GM00637 cells as a normal control, the cells were grown overnight and then treated with 2 mM hydroxyurea for 16 h. Cells were harvested and lysed and the protein concentrations in supernatants were determined as described previously (84). For each sample, equivalent amounts of proteins from whole cell lysates were loaded for separation by SDS-PAGE, followed by transfer to nitrocellulose, blocking, incubation with primary and secondary antibodies and detection by chemiluminescence as described previously (84). Primary antibodies included rabbit anti-FANCD2 (Novus, Centennial, CO, U.S.A., #NB100–182), rabbit anti-BRIP1/FANCJ (Abcam, ab49657) and mouse anti-actin (Santa Cruz Biotechnology, Dallas, Texas, U.S.A., sc-8432).

Foci analyses

RAD51 foci were analyzed in U2OS cells, as described previously (21). Briefly, 3×10^4 cells/well in 24-well plates were transfected the next day with 12 pmol of the appropriate mixture of miR-15a-5p, miR-544a and miR-494-3p mimics (composed of 4 pmol of each mimic), n.t.siRNA or a RAD51D specific siRNA using lipofectamine 2000 transfection reagent (Invitrogen (Thermo Fisher), Darmstadt, Germany). For comparability with the mimic mixture results, we also used 4 pmol of the appropriate mimics in transfections with single miRNA mimics. 48 h post transfection, cells were irradiated with 10 Gray, fixed 6 h after irradiation and then immunostained using a RAD51 antibody (Abcam ab133534) and analyzed for foci formation by immunofluorescence microscopy. Overall 700–1000 cells were counted for each transfection condition. Nuclei displaying ≥ five foci signals were counted as positive.

Homologous recombination assay

A total of 3×10^5 U2OS-DR cells/well in six-well plates were cotransfected with 20 pMol of the appropriate miRNA mimics and controls and 10 μg of I-*SceI* expression vector, ISceI-GR-RFP, (Addgene, Teddington, UK) using the lipofectamine 2000 transfection reagent (Invitrogen (Thermo Fisher), Darmstadt, Germany). Mock-transfected cells served as a control. Nuclear import of the nuclease I-SceI was induced by adding triamcinolone acetonide (TA) to a final concentration of 100 nM 48 h post transfection. For each transfection condition, 5×10^5 cells were analyzed by flow cytometry (CyAn ADP, Dako Cytomation, Beckman Coulter, Krefeld, Germany) for expression of GFP and dsRED 48 h after TA addition.

Supplementary Material

Supplementary Material is available at *HMG* online.

Acknowledgement

We would like to thank the FA patients and their families for supporting our research. We thank Jürgen Enczmann for assistance in data handling and Agathe Czapla for support in experimental target validations. We would like to thank Jörg Schipper,

Martin Wagenmann and Kathrin Scheckenbach for support of this research project.

Conflict of Interest statement. The authors declare no conflict of interests.

Funding

This work was supported by a grant from the Research Commission of the Medical Faculty, Heinrich Heine University Düsseldorf, given to H.I.T. and by a grant from the Deutsche Forschungsgemeinschaft (DFG, CW/2021–06) given to C.W. The work of H.H. was supported in part by the Essener Elterninitiative zur Unterstützung krebskranker Kinder e.V. This work was also supported by a National Institutes of Health grant (R01GM134731) to P.R.A.

References

1. Bartel, D.P. (2018) Metazoan microRNAs. *Cell*, **173**, 20–51.
2. Lim, L.P., Lau, N.C., Garrett-Engele, P., Grimson, A., Schelter, J.M., Castle, J., Bartel, D.P., Linsley, P.S. and Johnson, J.M. (2005) Microarray analysis shows that some microRNAs downregulate large numbers of target mRNAs. *Nature*, **433**, 769–773.
3. Lewis, B.P., Burge, C.B. and Bartel, D.P. (2005) Conserved seed pairing, often flanked by adenosines, indicates that thousands of human genes are microRNA targets. *Cell*, **120**, 15–20.
4. Lagos-Quintana, M., Rauhut, R., Yalcin, A., Meyer, J., Lendeckel, W. and Tuschl, T. (2002) Identification of tissue-specific microRNAs from mouse. *Curr. Biol.*, **12**, 735–739.
5. Sempere, L.F., Freemantle, S., Pitha-Rowe, I., Moss, E., Dmitrovsky, E. and Ambros, V. (2004) Expression profiling of mammalian microRNAs uncovers a subset of brain-expressed microRNAs with possible roles in murine and human neuronal differentiation. *Genome Biol.*, **5**, R13.
6. Subramanian, S. and Steer, C.J. (2010) MicroRNAs as gatekeepers of apoptosis. *J. Cell. Physiol.*, **223**, 289–298.
7. Shenouda, S.K. and Alahari, S.K. (2009) MicroRNA function in cancer: oncogene or a tumor suppressor? *Cancer Metast. Rev.*, **28**, 369–378.
8. Cai, X., Hagedorn, C.H. and Cullen, B.R. (2004) Human microRNAs are processed from capped, polyadenylated transcripts that can also function as mRNAs. *RNA*, **10**, 1957–1966.
9. Lee, Y., Jeon, K., Lee, J.T., Kim, S. and Kim, V.N. (2002) MicroRNA maturation: stepwise processing and subcellular localization. *EMBO J.*, **21**, 4663–4670.
10. Niraj, J., Farkkila, A. and D'Andrea, A.D. (2019) The Fanconi anemia pathway in cancer. *Annu. Rev. Cancer Biol.*, **3**, 457–478.
11. Kutler, D.I., Singh, B., Satagopan, J., Batish, S.D., Berwick, M., Giampietro, P.F., Hanenberg, H. and Auerbach, A.D. (2003) A 20-year perspective on the International Fanconi Anemia Registry (IFAR). *Blood*, **101**, 1249–1256.
12. Auerbach, A.D. (2009) Fanconi anemia and its diagnosis. *Mutat. Res.*, **668**, 4–10.
13. Semlow, D.R. and Walter, J.C. (2021) Mechanisms of vertebrate DNA interstrand cross-link repair. *Annu. Rev. Biochem.*, **90**, 107–135.
14. Virts, E.L., Jankowska, A., Mackay, C., Glaas, M.F., Wiek, C., Kelich, S.L., Lottmann, N., Kennedy, F.M., Marchal, C., Lehnert, E. *et al.* (2015) AluY-mediated germline deletion, duplication and somatic stem cell reversion in UBE2T defines a new subtype of Fanconi anemia. *Hum. Mol. Genet.*, **24**, 5093–5108.
15. Tarsounas, M. and Sung, P. (2020) The antitumorigenic roles of BRCA1-BARD1 in DNA repair and replication. *Nat. Rev. Mol. Cell Biol.*, **21**, 284–299.
16. Deans, A.J. and West, S.C. (2011) DNA interstrand crosslink repair and cancer. *Nat. Rev. Cancer*, **11**, 467–480.
17. Wyatt, H.D. and West, S.C. (2014) Holliday junction resolvases. *Cold Spring Harb. Perspect. Biol.*, **6**, a023192.
18. Bonilla, B., Hengel, S.R., Grundy, M.K. and Bernstein, K.A. (2020) RAD51 gene family structure and function. *Annu. Rev. Genet.*, **54**, 25–46.
19. Golmard, L., Castera, L., Krieger, S., Moncoutier, V., Abidallah, K., Tenreiro, H., Lauge, A., Tarabeux, J., Millot, G.A., Nicolas, A. *et al.* (2017) Contribution of germline deleterious variants in the RAD51 paralogs to breast and ovarian cancers. *Eur. J. Hum. Genet.*, **25**, 1345–1353.
20. Golmard, L., Caux-Moncoutier, V., Davy, G., Al Ageeli, E., Poirot, B., Tirapo, C., Michaux, D., Barbaroux, C., d'Enghien, C.D., Nicolas, A. *et al.* (2013) Germline mutation in the RAD51B gene confers predisposition to breast cancer. *BMC Cancer*, **13**, 484.
21. Meindl, A., Hellebrand, H., Wiek, C., Erven, V., Wappenschmidt, B., Niederacher, D., Freund, M., Lichtner, P., Hartmann, L., Schaal, H. *et al.* (2010) Germline mutations in breast and ovarian cancer pedigrees establish RAD51C as a human cancer susceptibility gene. *Nat. Genet.*, **42**, 410–414.
22. Loveday, C., Turnbull, C., Ramsay, E., Hughes, D., Ruark, E., Frankum, J.R., Bowden, G., Kalmyrzaev, B., Warren-Perry, M., Snape, K. *et al.* (2011) Germline mutations in RAD51D confer susceptibility to ovarian cancer. *Nat. Genet.*, **43**, 879–882.
23. Hilbers, F.S., Wijnen, J.T., Hoogerbrugge, N., Oosterwijk, J.C., Collee, M.J., Peterlongo, P., Radice, P., Manoukian, S., Feroce, I., Capra, F. *et al.* (2012) Rare variants in XRCC2 as breast cancer susceptibility alleles. *J. Med. Genet.*, **49**, 618–620.
24. Fragkos, M., Barra, V., Egger, T., Bordignon, B., Lemacon, D., Naim, V. and Coquelle, A. (2019) Dicer prevents genome instability in response to replication stress. *Oncotarget*, **10**, 4407–4423.
25. Suresh, B., Kumar, A.M., Jeong, H.S., Cho, Y.H., Ramakrishna, S. and Kim, K.S. (2015) Regulation of Fanconi anemia protein FANCD2 monoubiquitination by miR-302. *Biochem. Biophys. Res. Commun.*, **466**, 180–185.
26. Tsai, Y.S., Lin, C.S., Chiang, S.L., Lee, C.H., Lee, K.W. and Ko, Y.C. (2011) Areca nut induces miR-23a and inhibits repair of DNA double-strand breaks by targeting FANCG. *Toxicol. Sci.*, **123**, 480–490.
27. Garcia, A.I., Buisson, M., Bertrand, P., Rimokh, R., Rouleau, E., Lopez, B.S., Lidereau, R., Mikaelian, I. and Mazoyer, S. (2011) Down-regulation of BRCA1 expression by miR-146a and miR-146b-5p in triple negative sporadic breast cancers. *EMBO Mol. Med.*, **3**, 279–290.
28. Wang, Y., Huang, J.W., Calses, P., Kemp, C.J. and Taniguchi, T. (2012) MiR-96 downregulates REV1 and RAD51 to promote cellular sensitivity to cisplatin and PARP inhibition. *Cancer Res.*, **72**, 4037–4046.
29. Gasparini, P., Lovat, F., Fassan, M., Casadei, L., Cascione, L., Jacob, N.K., Carasi, S., Palmieri, D., Costinean, S., Shapiro, C.L. *et al.* (2014) Protective role of miR-155 in breast cancer through RAD51 targeting impairs homologous recombination after irradiation. *Proc. Natl. Acad. Sci. U. S. A.*, **111**, 4536–4541.
30. Cortez, M.A., Valdecanas, D., Niknam, S., Peltier, H.J., Diao, L., Giri, U., Komaki, R., Calin, G.A., Gomez, D.R., Chang, J.Y. *et al.* (2015) In vivo delivery of miR-34a sensitizes lung tumors to radiation through RAD51 regulation. *Mol. Ther. Nucleic Acids*, **4**, e270.
31. Huang, J.W., Wang, Y., Dhillon, K.K., Calses, P., Villegas, E., Mitchell, P.S., Tewari, M., Kemp, C.J. and Taniguchi, T. (2013)

Systematic screen identifies miRNAs that target RAD51 and RAD51D to enhance chemosensitivity. *Mol. Cancer Res.*, **11**, 1564–1573.
32. Duan, W., Tang, S., Gao, L., Dotts, K., Fink, A., Kalvala, A., Aguila, B., Wang, Q.E. and Villalona-Calero, M.A. (2021) MiRNA-200C expression in Fanconi anemia pathway functionally deficient lung cancers. *Sci. Rep.*, **11**, 4420.
33. Dweep, H. and Gretz, N. (2015) miRWalk2.0: a comprehensive atlas of microRNA-target interactions. *Nat. Methods*, **12**, 697.
34. Betel, D., Wilson, M., Gabow, A., Marks, D.S. and Sander, C. (2008) The microRNA.org resource: targets and expression. *Nucleic Acids Res.*, **36**, D149–D153.
35. Krek, A., Grun, D., Poy, M.N., Wolf, R., Rosenberg, L., Epstein, E.J., MacMenamin, P., da Piedade, I., Gunsalus, K.C., Stoffel, M. *et al.* (2005) Combinatorial microRNA target predictions. *Nat. Genet.*, **37**, 495–500.
36. Agarwal, V., Bell, G.W., Nam, J.W. and Bartel, D.P. (2015) Predicting effective microRNA target sites in mammalian mRNAs. *elife*, **4**, 38. https://doi.org/10.7554/eLife.05005.
37. Liu, W. and Wang, X. (2019) Prediction of functional microRNA targets by integrative modeling of microRNA binding and target expression data. *Genome Biol.*, **20**, 18.
38. Miranda, K.C., Huynh, T., Tay, Y., Ang, Y.S., Tam, W.L., Thomson, A.M., Lim, B. and Rigoutsos, I. (2006) A pattern-based method for the identification of MicroRNA binding sites and their corresponding heteroduplexes. *Cell*, **126**, 1203–1217.
39. Iwaniuk, K.M., Schira, J., Weinhold, S., Jung, M., Adjaye, J., Muller, H.W., Wernet, P. and Trompeter, H.I. (2011) Network-like impact of MicroRNAs on neuronal lineage differentiation of unrestricted somatic stem cells from human cord blood. *Stem Cells Dev.*, **20**, 1383–1394.
40. Trompeter, H.I., Abbad, H., Iwaniuk, K.M., Hafner, M., Renwick, N., Tuschl, T., Schira, J., Muller, H.W. and Wernet, P. (2011) MicroRNAs MiR-17, MiR-20a, and MiR-106b act in concert to modulate E2F activity on cell cycle arrest during neuronal lineage differentiation of USSC. *PLoS One*, **6**, e16138.
41. Trompeter, H.I., Dreesen, J., Hermann, E., Iwaniuk, K.M., Hafner, M., Renwick, N., Tuschl, T. and Wernet, P. (2013) MicroRNAs miR-26a, miR-26b, and miR-29b accelerate osteogenic differentiation of unrestricted somatic stem cells from human cord blood. *BMC Genomics*, **14**, 111.
42. Graffmann, N., Ring, S., Kawala, M.A., Wruck, W., Ncube, A., Trompeter, H.I. and Adjaye, J. (2016) Modeling nonalcoholic fatty liver disease with human pluripotent stem cell-derived immature hepatocyte-like cells reveals activation of PLIN2 and confirms regulatory functions of peroxisome proliferator-activated receptor alpha. *Stem Cells Dev.*, **25**, 1119–1133.
43. Gross, M., Hanenberg, H., Lobitz, S., Friedl, R., Herterich, S., Dietrich, R., Gruhn, B., Schindler, D. and Hoehn, H. (2002) Reverse mosaicism in Fanconi anemia: natural gene therapy via molecular self-correction. *Cytogenet. Genome Res.*, **98**, 126–135.
44. Nalepa, G., Enzor, R., Sun, Z., Marchal, C., Park, S.J., Yang, Y., Tedeschi, L., Kelich, S., Hanenberg, H. and Clapp, D.W. (2013) Fanconi anemia signaling network regulates the spindle assembly checkpoint. *J. Clin. Invest.*, **123**, 3839–3847.
45. Glaas, M.F., Wiek, C., Wolter, L.M., Roellecke, K., Balz, V., Okpanyi, V., Wagenmann, M., Hoffmann, T.K., Grässlin, R., Plettenberg, C. *et al.* (2018) Mutational and functional analysis of FANCB as a candidate gene for sporadic head and neck squamous cell carcinomas. *Anticancer Res.*, **38**, 1317–1325.
46. Sims, A.E., Spiteri, E., Sims, R.J., 3rd, Arita, A.G., Lach, F.P., Landers, T., Wurm, M., Freund, M., Neveling, K., Hanenberg, H. *et al.* (2007) FANCI is a second monoubiquitinated member of the Fanconi anemia pathway. *Nat. Struct. Mol. Biol.*, **14**, 564–567.
47. Colnaghi, L., Jones, M.J., Cotto-Rios, X.M., Schindler, D., Hanenberg, H. and Huang, T.T. (2011) Patient-derived C-terminal mutation of FANCI causes protein mislocalization and reveals putative EDGE motif function in DNA repair. *Blood*, **117**, 2247–2256.
48. Levran, O., Attwooll, C., Henry, R.T., Milton, K.L., Neveling, K., Rio, P., Batish, S.D., Kalb, R., Velleuer, E., Barral, S. *et al.* (2005) The BRCA1-interacting helicase BRIP1 is deficient in Fanconi anemia. *Nat. Genet.*, **37**, 931–933.
49. Barthelemy, J., Hanenberg, H. and Leffak, M. (2016) FANCJ is essential to maintain microsatellite structure genome-wide during replication stress. *Nucleic Acids Res.*, **44**, 6803–6816.
50. Ameziane, N., May, P., Haitjema, A., van de Vrugt, H.J., van Rossum-Fikkert, S.E., Ristic, D., Williams, G.J., Balk, J., Rockx, D., Li, H. *et al.* (2015) A novel Fanconi anaemia subtype associated with a dominant-negative mutation in RAD51. *Nat. Commun.*, **6**, 8829.
51. Vaz, F., Hanenberg, H., Schuster, B., Barker, K., Wiek, C., Erven, V., Neveling, K., Endt, D., Kesterton, I., Autore, F. *et al.* (2010) Mutation of the RAD51C gene in a Fanconi anemia-like disorder. *Nat. Genet.*, **42**, 406–409.
52. The Gene Ontology, C (2019) The gene ontology resource: 20 years and still going strong. *Nucleic Acids Res.*, **47**, D330–D338.
53. Huang da, W., Sherman, B.T. and Lempicki, R.A. (2009) Systematic and integrative analysis of large gene lists using DAVID bioinformatics resources. *Nat. Protoc.*, **4**, 44–57.
54. Huang da, W., Sherman, B.T. and Lempicki, R.A. (2009) Bioinformatics enrichment tools: paths toward the comprehensive functional analysis of large gene lists. *Nucleic Acids Res.*, **37**, 1–13.
55. Gunn, A. and Stark, J.M. (2012) I-SceI-based assays to examine distinct repair outcomes of mammalian chromosomal double strand breaks. *Methods Mol. Biol.*, **920**, 379–391.
56. Pierce, A.J., Johnson, R.D., Thompson, L.H. and Jasin, M. (1999) XRCC3 promotes homology-directed repair of DNA damage in mammalian cells. *Genes Dev.*, **13**, 2633–2638.
57. Thapar, R. (2018) Regulation of DNA double-strand break repair by non-coding RNAs. *Molecules*, **23**, 23. https://doi.org/10.3390/molecules23112789.
58. D'Andrea, A.D. (2010) Susceptibility pathways in Fanconi's anemia and breast cancer. *N. Engl. J. Med.*, **362**, 1909–1919.
59. Chen, S., Liu, R., Wang, Q., Qi, Z., Hu, Y., Zhou, P. and Wang, Z. (2019) MiR-34s negatively regulate homologous recombination through targeting RAD51. *Arch. Biochem. Biophys.*, **666**, 73–82.
60. Choi, Y.E., Pan, Y., Park, E., Konstantinopoulos, P., De, S., D'Andrea, A. and Chowdhury, D. (2014) MicroRNAs down-regulate homologous recombination in the G1 phase of cycling cells to maintain genomic stability. *elife*, **3**, e02445.
61. Liu, G., Xue, F. and Zhang, W. (2015) miR-506: a regulator of chemo-sensitivity through suppression of the RAD51-homologous recombination axis. *Chin. J. Cancer*, **34**, 485–487.
62. Rojas, E., Martinez-Pacheco, M., Rodriguez-Sastre, M.A., Ramos-Espinosa, P. and Valverde, M. (2020) Post-transcriptional regulation of Rad51c by miR-222 contributes cellular transformation. *PLoS One*, **15**, e0221681.
63. Li, Y., Hu, G., Li, P., Tang, S., Zhang, J. and Jia, G. (2016) miR-3940-5p enhances homologous recombination after DSB in Cr(VI) exposed 16HBE cell. *Toxicology*, **344-346**, 1–6.
64. Schira-Heinen, J., Czapla, A., Hendricks, M., Kloetgen, A., Wruck, W., Adjaye, J., Kögler, G., Werner Müller, H., Stühler, K. and Trompeter, H.I. (2020) Functional omics analyses reveal only

minor effects of microRNAs on human somatic stem cell differentiation. *Sci. Rep.*, **10**, 3284.
65. Park, J.Y., Virts, E.L., Jankowska, A., Wiek, C., Othman, M., Chakraborty, S.C., Vance, G.H., Alkuraya, F.S., Hanenberg, H. and Andreassen, P.R. (2016) Complementation of hypersensitivity to DNA interstrand crosslinking agents demonstrates that XRCC2 is a Fanconi anaemia gene. *J. Med. Genet.*, **53**, 672–680.
66. Reid, S., Schindler, D., Hanenberg, H., Barker, K., Hanks, S., Kalb, R., Neveling, K., Kelly, P., Seal, S., Freund, M. *et al.* (2007) Biallelic mutations in PALB2 cause Fanconi anemia subtype FA-N and predispose to childhood cancer. *Nat. Genet.*, **39**, 162–164.
67. Sullivan, M.R. and Bernstein, K.A. (2018) RAD-ical new insights into RAD51 regulation. *Genes (Basel)*, **9**, 23. https://doi.org/10.3390/genes9120629.
68. O'Donnell, L., Panier, S., Wildenhain, J., Tkach, J.M., Al-Hakim, A., Landry, M.C., Escribano-Diaz, C., Szilard, R.K., Young, J.T., Munro, M. *et al.* (2010) The MMS22L-TONSL complex mediates recovery from replication stress and homologous recombination. *Mol. Cell*, **40**, 619–631.
69. Espinosa-Diez, C., Wilson, R., Chatterjee, N., Hudson, C., Ruhl, R., Hipfinger, C., Helms, E., Khan, O.F., Anderson, D.G. and Anand, S. (2018) MicroRNA regulation of the MRN complex impacts DNA damage, cellular senescence, and angiogenic signaling. *Cell Death Dis.*, **9**, 632.
70. Symington, L.S. and Gautier, J. (2011) Double-strand break end resection and repair pathway choice. *Annu. Rev. Genet.*, **45**, 247–271.
71. Bernstein, K.A. and Rothstein, R. (2009) At loose ends: resecting a double-strand break. *Cell*, **137**, 807–810.
72. Zhang, Q., Li, Y., Zhao, M., Lin, H., Wang, W., Li, D., Cui, W., Zhou, C., Zhong, J. and Huang, C. (2019) MiR-494 acts as a tumor promoter by targeting CASP2 in non-small cell lung cancer. *Sci. Rep.*, **9**, 3008.
73. Zhu, L., Wang, X., Wang, T., Zhu, W. and Zhou, X. (2019) miR-494-3p promotes the progression of endometrial cancer by regulating the PTEN/PI3K/AKT pathway. *Mol. Med. Rep.*, **19**, 581–588.
74. Faversani, A., Amatori, S., Augello, C., Colombo, F., Porretti, L., Fanelli, M., Ferrero, S., Palleschi, A., Pelicci, P.G., Belloni, E. *et al.* (2017) miR-494-3p is a novel tumor driver of lung carcinogenesis. *Oncotarget*, **8**, 7231–7247.
75. Macedo, T., Silva-Oliveira, R.J., Silva, V.A.O., Vidal, D.O., Evangelista, A.F. and Marques, M.M.C. (2017) Overexpression of mir-183 and mir-494 promotes proliferation and migration in human breast cancer cell lines. *Oncol. Lett.*, **14**, 1054–1060.
76. Alblihy, A., Shoqafi, A., Toss, M.S., Algethami, M., Harris, A.E., Jeyapalan, J.N., Abdel-Fatah, T., Servante, J., Chan, S.Y.T., Green, A. *et al.* (2021) Untangling the clinicopathological significance of MRE11-RAD50-NBS1 complex in sporadic breast cancers. *NPJ Breast Cancer*, **7**, 143.
77. Xiang, Z., Sun, M., Yuan, Z., Zhang, C., Jiang, J., Huang, S. and Xiong, B. (2018) Prognostic and clinicopathological significance of microRNA-494 overexpression in cancers: a meta-analysis. *Oncotarget*, **9**, 1279–1290.
78. Chava, S., Reynolds, C.P., Pathania, A.S., Gorantla, S., Poluektova, L.Y., Coulter, D.W., Gupta, S.C., Pandey, M.K. and Challagundla, K.B. (2020) miR-15a-5p, miR-15b-5p, and miR-16-5p inhibit tumor progression by directly targeting MYCN in neuroblastoma. *Mol. Oncol.*, **14**, 180–196.
79. Wang, Z.M., Wan, X.H., Sang, G.Y., Zhao, J.D., Zhu, Q.Y. and Wang, D.M. (2017) miR-15a-5p suppresses endometrial cancer cell growth via Wnt/β-catenin signaling pathway by inhibiting WNT3A. *Eur. Rev. Med. Pharmacol. Sci.*, **21**, 4810–4818.
80. Stella di Stadio, C., Faraonio, R., Federico, A., Altieri, F., Rippa, E. and Arcari, P. (2019) GKN1 expression in gastric cancer cells is negatively regulated by miR-544a. *Biochimie*, **167**, 42–48.
81. Yanaka, Y., Muramatsu, T., Uetake, H., Kozaki, K. and Inazawa, J. (2015) miR-544a induces epithelial-mesenchymal transition through the activation of WNT signaling pathway in gastric cancer. *Carcinogenesis*, **36**, 1363–1371.
82. Wang, Y., Bao, W., Liu, Y., Wang, S., Xu, S., Li, X., Li, Y. and Wu, S. (2018) miR-98-5p contributes to cisplatin resistance in epithelial ovarian cancer by suppressing miR-152 biogenesis via targeting Dicer1. *Cell Death Dis.*, **9**, 447.
83. Chen, C., Ridzon, D.A., Broomer, A.J., Zhou, Z., Lee, D.H., Nguyen, J.T., Barbisin, M., Xu, N.L., Mahuvakar, V.R., Andersen, M.R. *et al.* (2005) Real-time quantification of microRNAs by stem-loop RT-PCR. *Nucleic Acids Res.*, **33**, e179.
84. Fan, Q., Zhang, F., Barrett, B., Ren, K. and Andreassen, P.R. (2009) A role for monoubiquitinated FANCD2 at telomeres in ALT cells. *Nucleic Acids Res.*, **37**, 1740–1754.